Supplementary Figures

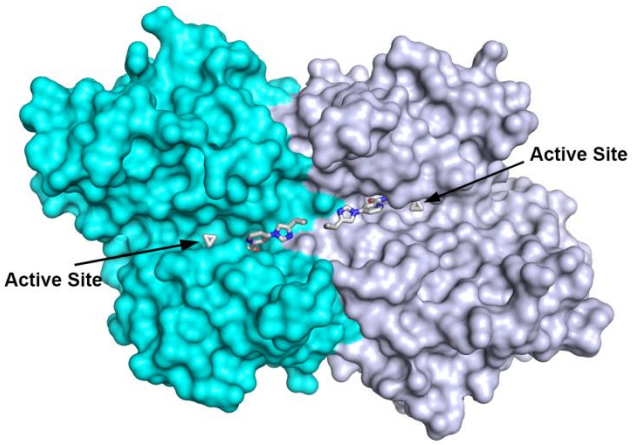

Supplementary Figure 1. **Compound 3 (GS-444217), a selective ATP-competitive inhibitor of ASK1.** Structure of the ASK1 homodimer with compound **3** bound in the active site. The active sites from each monomer are facing towards each other, and the cyclopropyl groups are within 3.3 Å of each other.

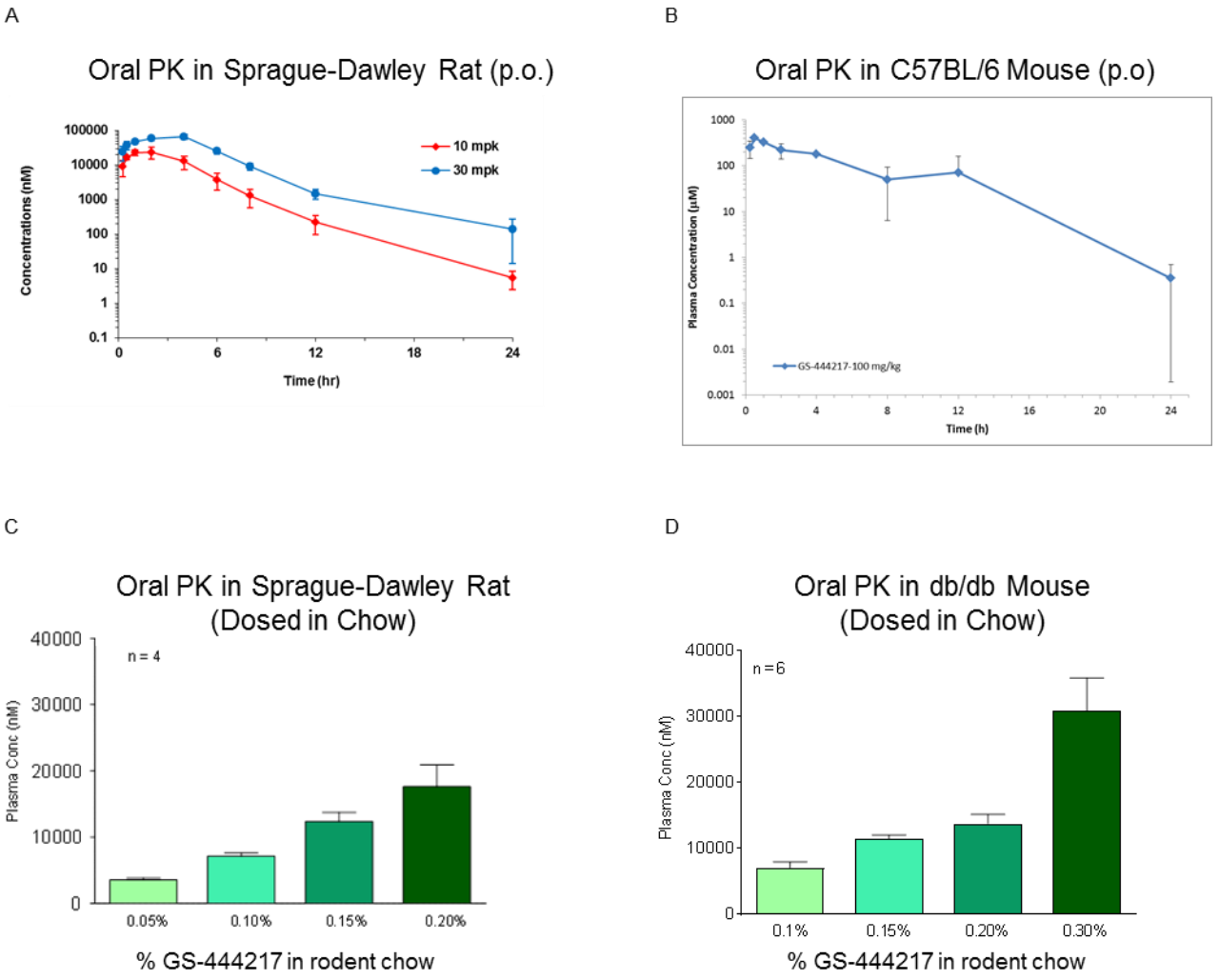

Supplementary Figure 2. **Pharmacokinetics (PK) of GS-444217 in rats and mice following oral administration.** (**A,B**) GS-444217 plasma concentrations vs. time following a single oral gavage (p.o.) of (**A**) 10 or 30 mg/kg to non-fasted Sprague-Dawley rats (mean ± SD, n = 3 per group) or (**B**) 100 mg/kg to non-fasted C57BL/6 mice (mean ± SD, n = 3). (C,**D**) GS-444217 plasma concentrations vs. dose of GS-444217 fed in standard rodent chow ((0.05-0.3% by weight; Purina 5001, Research Diets, Inc.) measured after 4 days of treatment in (**C**) Sprague-Dawley rats (n = 4 per group) or (**D**) db/db mice (n = 6 per group). Concentrations of GS-444217 were measured in plasma by HPLC coupled to tandem mass spectrometry.

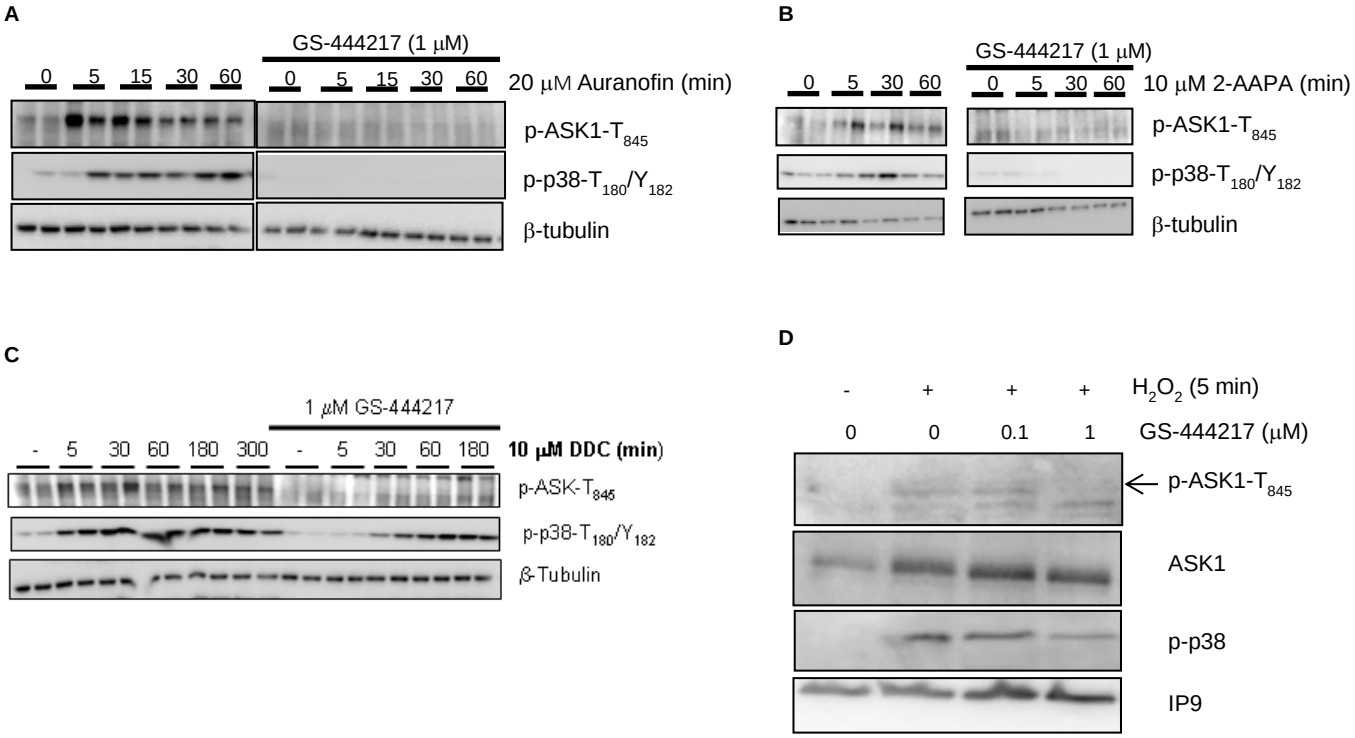

Supplementary Figure 3. **GS-444217 blocks oxidation-induced ASK1 activation in vitro. (A-D)** Chemical inhibitors of the antioxidant proteins were tested for their ability to induce sustained activation of the ASK1 pathway (ASK1-T845 autophosphorylation and p38-T180/Y181 phosphorylation measured by Western blotting) in vitro. (**A-C**) Time courses with addition of antioxidant inhibitors and pretreatment of neonatal rat ventricular myocytes with 1 μM GS-444217 (β-tubulin was used as a protein loading control): (**A**) 20 μM auranofin (thioredoxin reductase inhibitor). ASK1 and p38 phosphorylation could not be assessed at 60 min post-auranofin treatment because extensive cell death occurred (data not shown) leading to a reduction of total protein levels indicated by a low β-tubulin signal; (**B**) 10 μM 2-AAPA (glutaredoxin inhibitor); or (**C**) 20 μM DDC (superoxide dismutase inhibitor). (**D**) Inhibition of ASK1 pathway activation was tested in HK-2 cells (immortalized proximal tubule epithelial cell line) pretreated with 0.1 or 1 μM of GS-444217 followed by treatment with 1 μM H_2O_2 for 5 min. IP90 was used as a protein loading control.

A

BioMAP® Diversity PLUS Panel

System	Relevance	Cell Type	Biomarker Readout
/Mphg	Cardiovascular Disease, Chronic Inflammation, Restenosis	Macrophages + Venular endothelial cells	CCL2/MCP-1, CCL3/MIP-1 α, CD106/VCAM-1, CD40, CD62E/E-Selectin, CD69, CXCL8/IL-8, IL-1 α, M-CSF, sIL-10, SRB, SRB-Mphg
3C	Cardiovascular Disease, Chronic Inflammation	Venular endothelial cells	CCL2/MCP-1, CD106/VCAM-1, CD141/Thrombomodulin, CD142/Tissue Factor, CD54/ICAM-1, CD62E/E-Selectin, CD87/uPAR, CXCL8/IL-8, CXCL9/MIG, HLA-DR, Proliferation, SRB
4H	Allergy, Asthma, Autoimmunity	Venular endothelial cells	CCL2/MCP-1, CCL26/Eotaxin-3, CD106/VCAM-1, CD62P/P-Selectin, CD87/uPAR, SRB, VEGFR2
BE3C	COPD, Lung Inflammation	Bronchial epithelial cells	CD54/ICAM-1, CD87/uPAR, CXCL10/IP-10, CXCL11/I-TAC, CXCL8/IL-8, CXCL9/MIG, EGFR, HLA-DR, IL-1 α, Keratin 8/18, MMP-1, MMP-9, PAI-I, SRB, tPA, uPA
BF4T	Allergy, Asthma, Fibrosis, Lung Inflammation	Bronchial epithelial cells + Dermal fibroblasts	CCL2/MCP-1, CCL26/Eotaxin-3, CD106/VCAM-1, CD54/ICAM-1, CD90, CXCL8/IL-8, IL-1 α, Keratin 8/18, MMP-1, MMP-3, MMP-9, PAI-I, SRB, tPA, uPA
BT	Allergy, Asthma, Autoimmunity, Oncology	B cells + Peripheral blood mononuclear cells	B cell Proliferation, PBMC Cytotoxicity, Secreted IgG, sIL-17A, sIL-17F, sIL-2, sIL-6, sTNF-α
CASM3C	Cardiovascular Inflammation, Restenosis	Coronary artery smooth muscle cells	CCL2/MCP-1, CD106/VCAM-1, CD141/Thrombomodulin, CD142/Tissue Factor, CD87/uPAR, CXCL8/IL-8, CXCL9/MIG, HLA-DR, IL-6, LDLR, M-CSF, PAI-I, Proliferation, Serum Amyloid A, SRB
HDF3CGF	Chronic Inflammation, Fibrosis	Dermal fibroblasts	CCL2/MCP-1, CD106/VCAM-1, CD54/ICAM-1, Collagen I, Collagen III, CXCL10/IP-10, CXCL11/I-TAC, CXCL8/IL-8, CXCL9/MIG, EGFR, M-CSF, MMP-1, PAI-I, Proliferation_72hr, SRB, TIMP-1, TIMP-2
KF3CT	Dermatitis, Psoriasis	Dermal fibroblasts + Keratinocytes	CCL2/MCP-1, CD54/ICAM-1, CXCL10/IP-10, CXCL8/IL-8, CXCL9/MIG, IL-1 α, MMP-9, PAI-I, SRB, TIMP-2, uPA
LPS	Cardiovascular Disease, Chronic Inflammation	Peripheral blood mononuclear cells + Venular endothelial cells	CCL2/MCP-1, CD106/VCAM-1, CD141/Thrombomodulin, CD142/Tissue Factor, CD40, CD62E/E-Selectin, CD69, CXCL8/IL-8, IL-1 α, M-CSF, sPGE2, SRB, sTNF-α
MyoF	Chronic Inflammation, Fibrosis, Matrix Remodeling, Wound Healing	Lung fibroblasts	bFGF, CD106/VCAM-1, Collagen I, Collagen III, Collagen IV, CXCL8/IL-8, Decorin, MMP-1, PAI-I, SRB, TIMP-1, α-SM Actin
SAg	Autoimmune Disease, Chronic Inflammation	Peripheral blood mononuclear cells + Venular endothelial cells	CCL2/MCP-1, CD38, CD40, CD62E/E-Selectin, CD69, CXCL8/IL-8, CXCL9/MIG, PBMC Cytotoxicity, Proliferation, SRB

B

BioMAP® Profiles of GS-444217 and BIRB-796

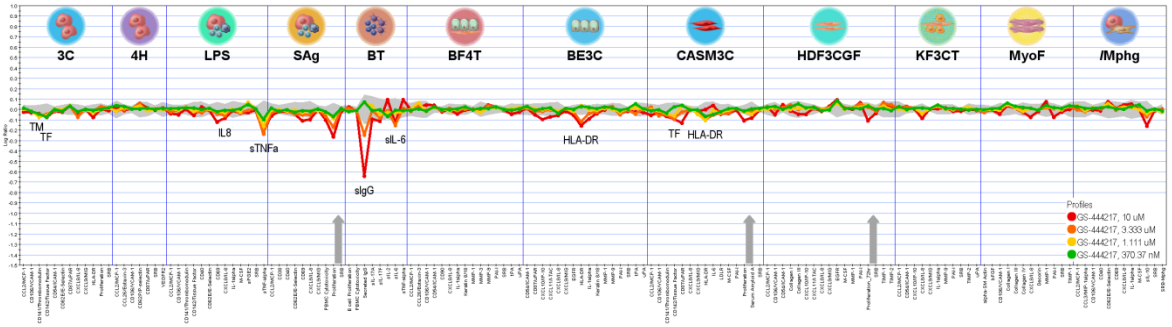

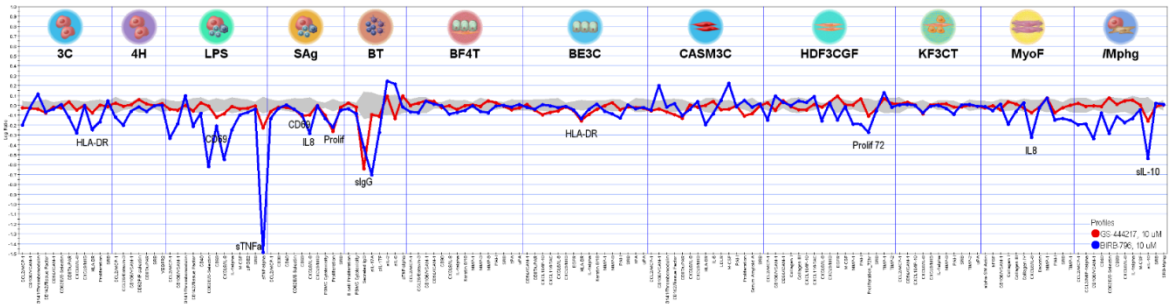

Supplementary Figure 4. **Profile of GS-44217 using the BioMAP® Diversity PLUS panel.**
(**A**) The activity of GS-444217 was evaluated in a panel of assays representing a broad range of biological processes in primary human cells using the BioMAP® Diversity PLUS panel. The panel consists of 12 BioMAP Systems containing early passage primary human cell types from multiple tissues. Cells are cultured alone or as co-cultures and stimulated with a combination of factors to recapitulate the multi-component signaling networks associated with disease states. (**B, upper panel**) GS-444217 was tested at 10 μM (red line), 3.333 μM (orange line), 1.111 μM (yellow line), and 370.37 nM (green line). (**B, lower panel**) The activity of 10 μM of GS-444217 (red line) was directly compared to 10 μM BIRB-796 (blue line), a selective p38 inhibitor.

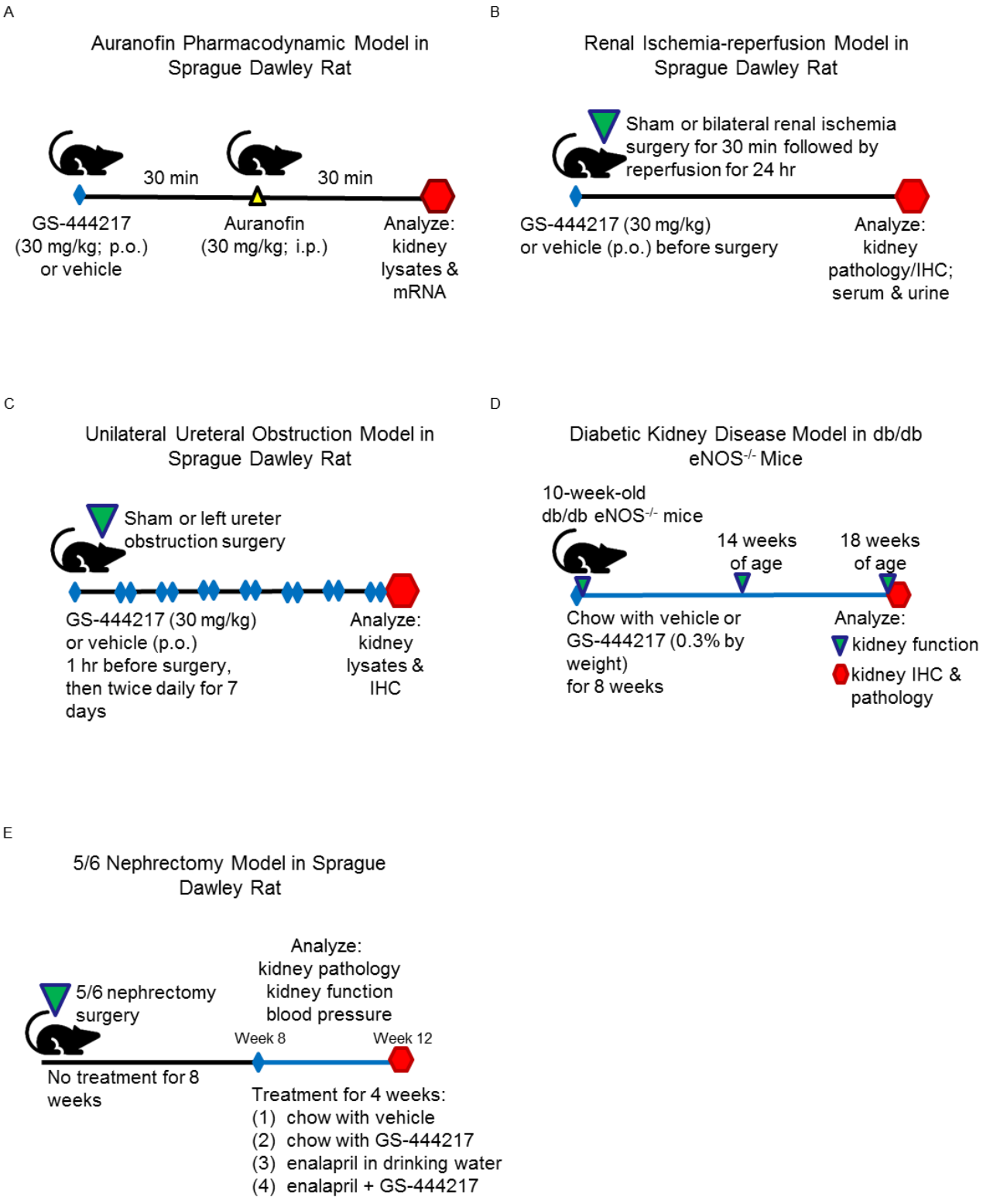

Supplementary Figure 5. Experimental outlines of pharmacodynamic and kidney injury models in rodents.

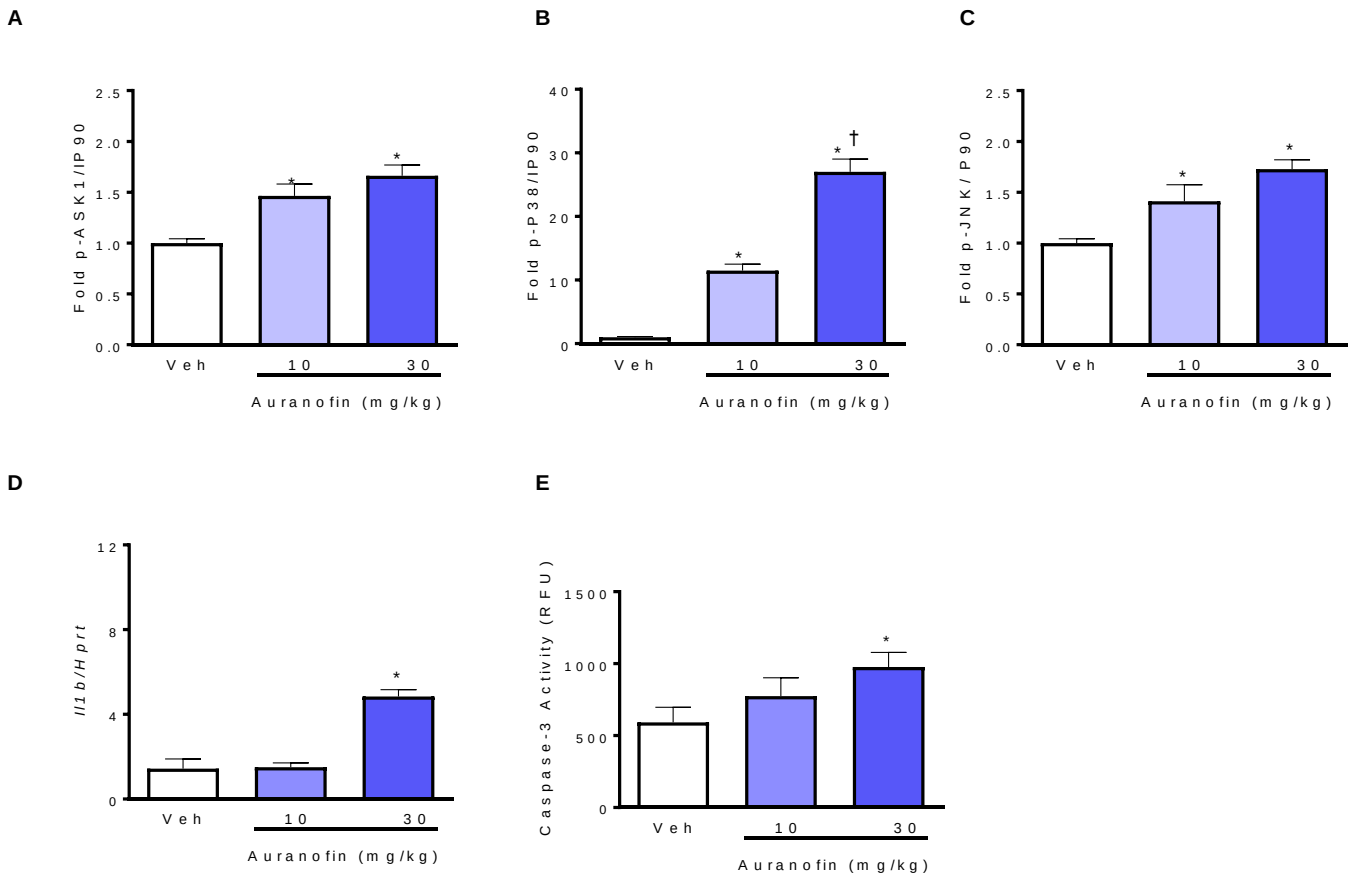

Supplementary Figure 6. **Auranofin induces endogenous ASK1 signaling in rat kidney.** (**A-E**) To establish proof-of-mechanism for an ASK1 inhibitor, an acute pharmacodynamic model was developed using an inhibitor of thioredoxin reductase, auranofin, which causes ASK1 activation. Sprague-Dawley rats were administered vehicle (veh, equal volume, i.p.) or auranofin (10 or 30 mg/kg, i.p.), and renal cortex lysates were quantitated 30 min later by Western blot for p-ASK1 (**A**) and its downstream targets p-p38 (**B**) and p-JNK (**C**) by Western blot. (**D**) Kidney expression of *Il1b* mRNA was assessed by real-time RT-PCR. (**E**) Caspase-3 activity was assessed by fluorescence. Data are mean ± SEM, n = 8; **P* < 0.05 vs. vehicle, †*P* < 0.05 vs. 10 mg/kg auranofin (ANOVA with Newman-Keuls multiple comparison test).

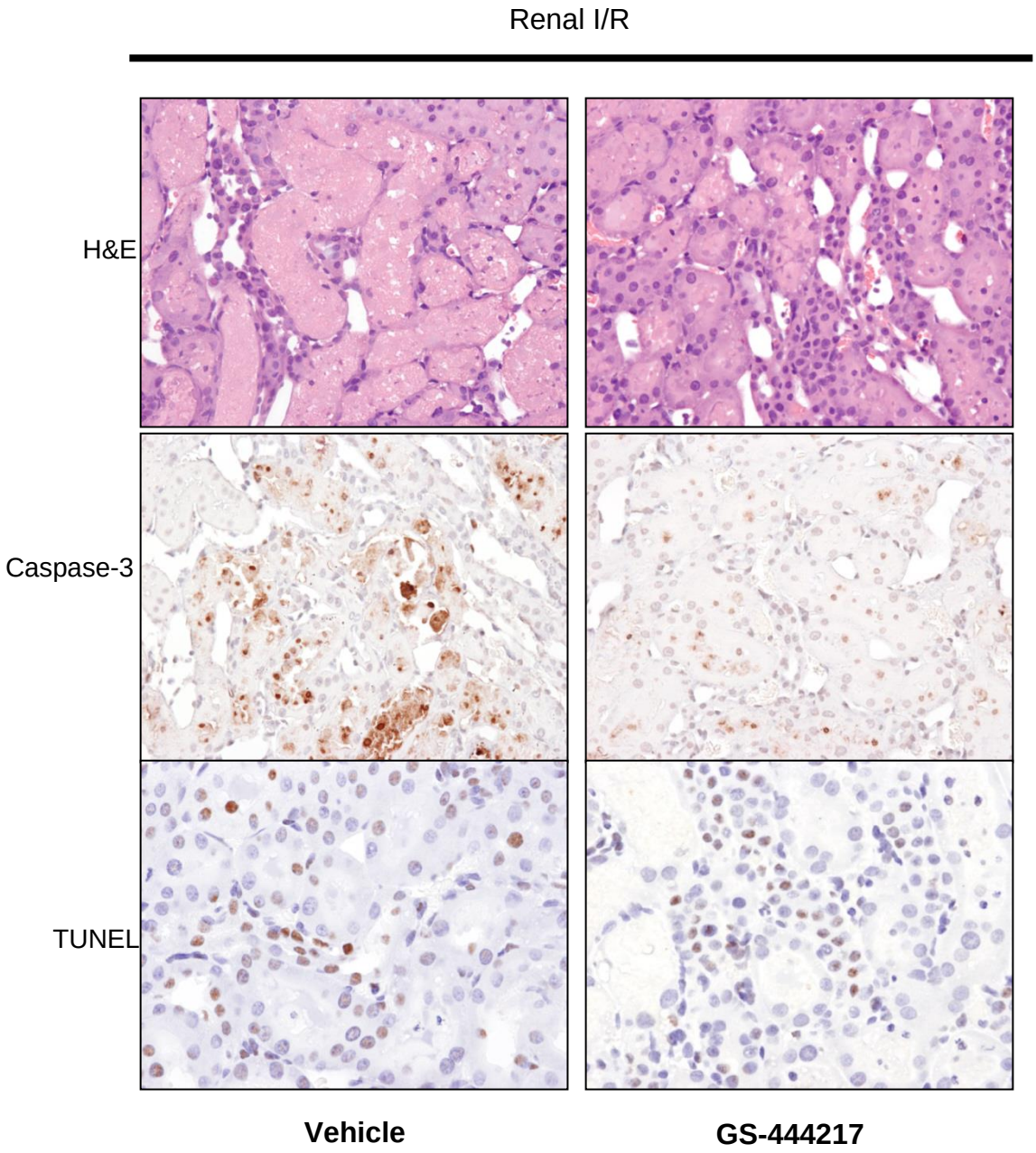

Supplementary Figure 7: GS-444217 reduces tubular fibrosis and renal cell death following ischemia reperfusion injury. GS-444217 (30 mg/kg) was orally administered to Sprague-Dawley rats immediately before 30 min of bilateral renal ischemia, and rats were evaluated following a 24-hr reperfusion period. Representative photomicrographs of kidney sections stained with H&E, for caspase-3 activity, and for apoptosis with TUNEL (400x and 600x magnification).

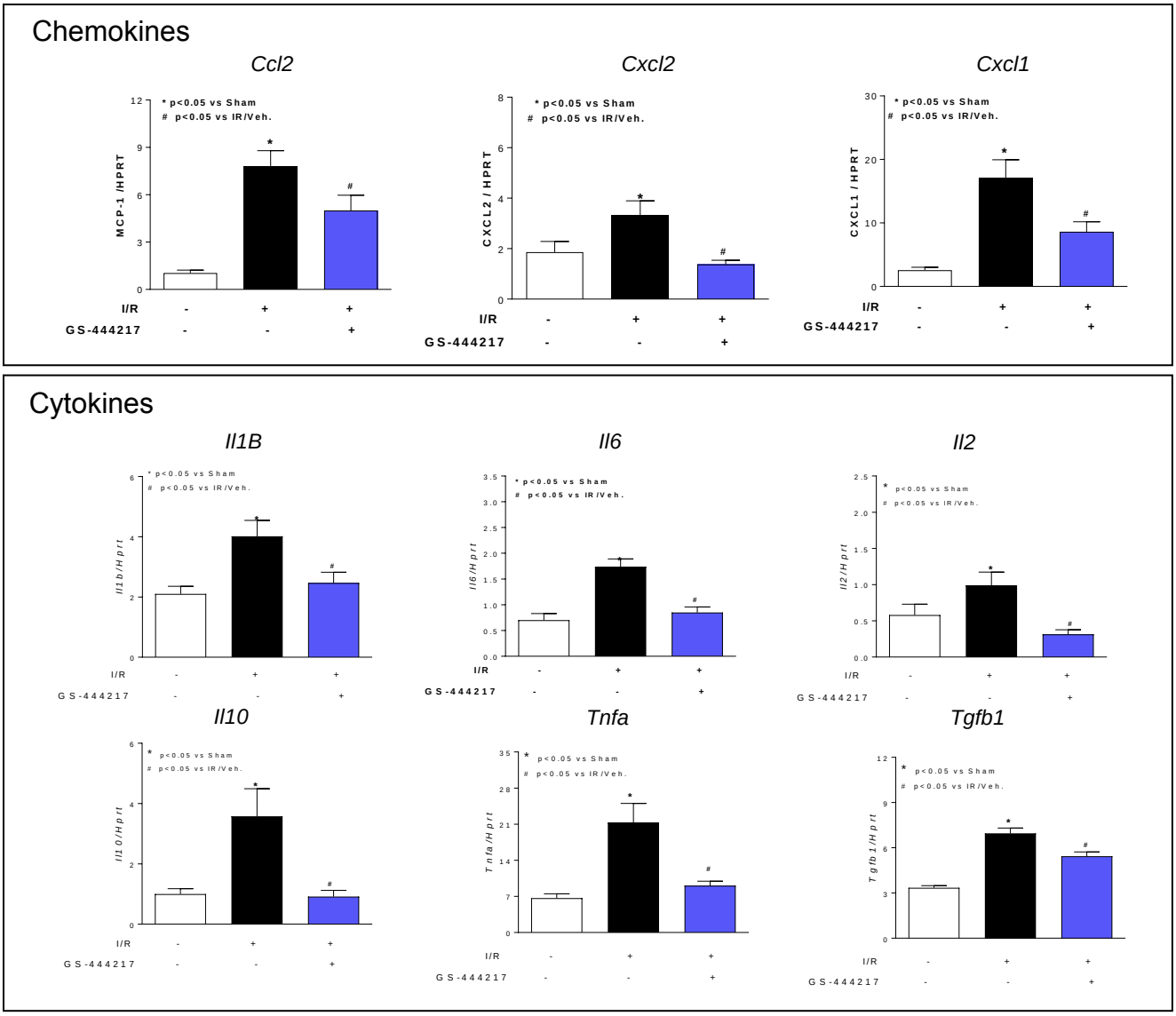

Supplementary Figure 8. **GS-444217 prevents expression of renal chemokines and cytokines following ischemia reperfusion injury**. GS-444217 (30 mg/kg) was orally administered to Sprague-Dawley rats immediately before 30 min of bilateral renal ischemia, and rats were evaluated following a 24-hr reperfusion period. Relative expression of kidney transcripts for *Ccl2*, *Cxcl2*, *Cxcl1*, *Il1b*, *Il6*, *Il2*, *Il10*, *Tnfa*, and *Tgfb1* mRNA was measured by Luminex. Data are mean ± SEM, n = 5 (sham surgery) and n = 8 (renal I/R surgery); **P* < 0.05 vs. sham, †*P* < 0.05 vs. I/R + vehicle (ANOVA with by Newman-Keuls multiple comparison test).

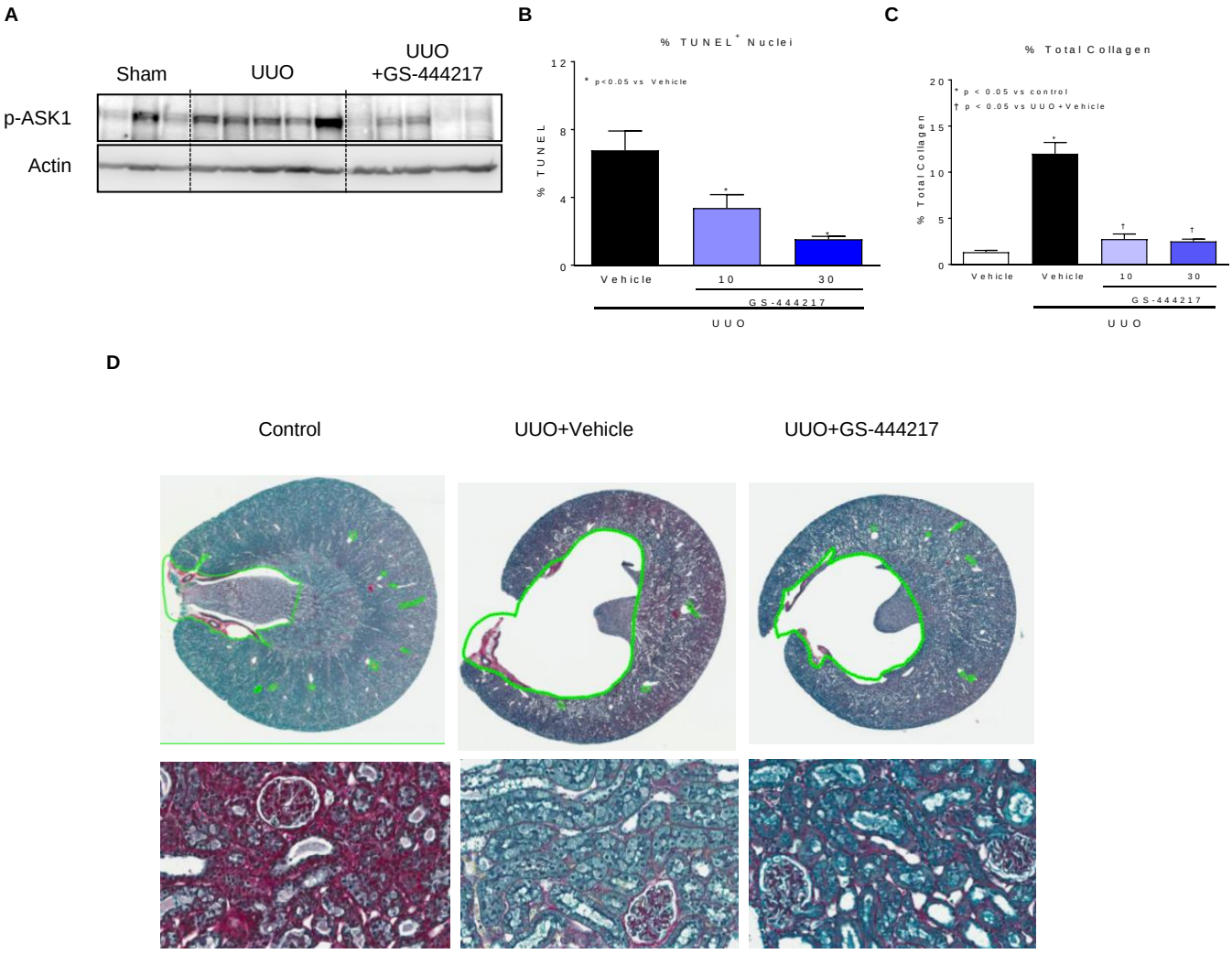

Supplementary Figure 9: GS-444217 decreases (A) ASK1 activation as measured by p-ASK1, (B) apoptosis as measured by TUNEL positive cells, (C) total collagen, and (D) interstitial fibrosis assessed on Masson's trichrome-stained sections following unilateral ureteral obstruction (UUO) in the rat. Sprague-Dawley rats underwent UUO or sham surgery. Treatment with GS-444217 (10 or 30 mg/kg, twice daily, orally) or vehicle (twice daily, orally) began 1 hour before surgery and continued for 7 days. Data are mean ± SEM, n = 5 (sham surgery), n = 5-8 (UUO surgery); *$P < 0.01$ vs. sham surgery; $^{\#}P < 0.01$ vs. UUO treated with vehicle (ANOVA with Bonferroni's multiple comparison test).

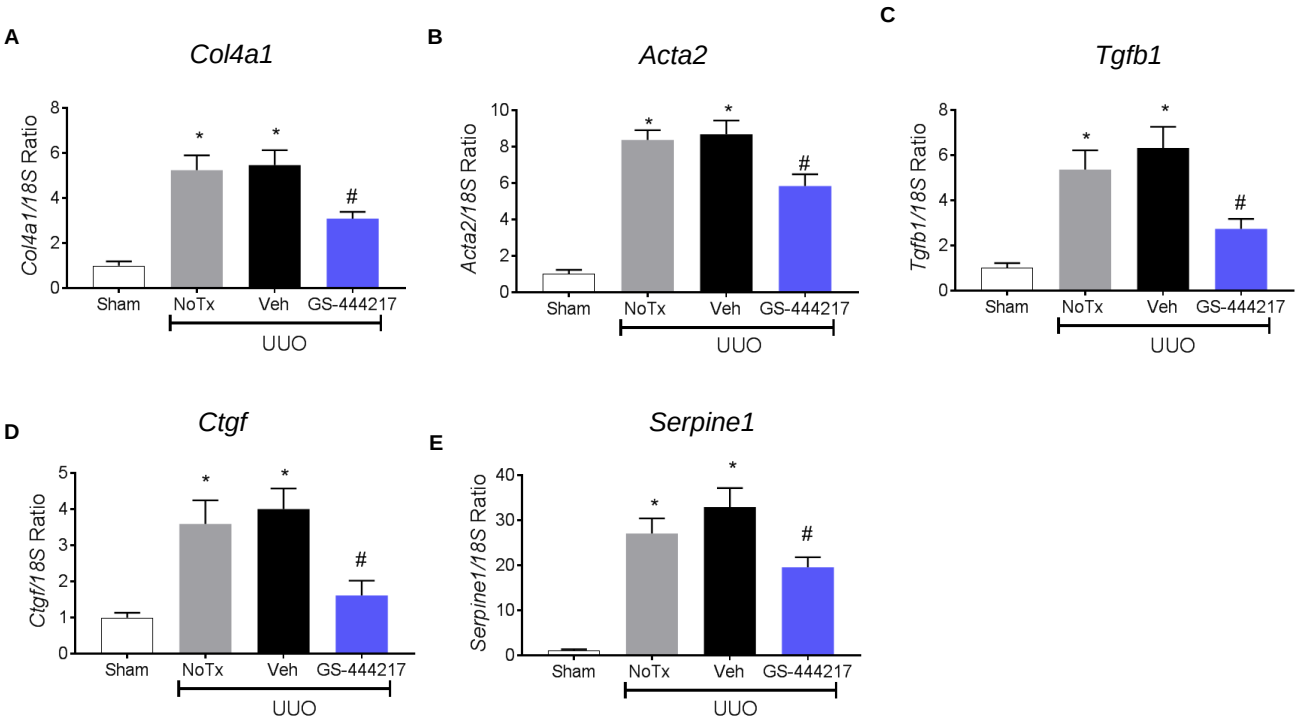

Supplementary Figure 10: GS-444217 inhibits expression of fibrotic genes following unilateral ureteral obstruction (UUO) in the rat. (**A**-**E**) Sprague-Dawley rats underwent UUO or sham surgery. Treatment with GS-444217 (30 mg/kg, twice daily, orally) or vehicle (twice daily, orally) began 1 hour before surgery and continued for 7 days. Relative expression of kidney transcripts for collagen IV (*Col4a1*) (**A**), alpha smooth muscle actin (*Acta1*) (**B**), transforming growth factor beta 1 (*Tgfb1*) (**C**), connective tissue growth factor (*Ctgf*), and (**D**) plasminogen activator inhibitor 1 (*Serpine1*) (**E**) mRNA was measured by RT-PCR. Data are mean ± SEM, n = 4 (sham surgery), n = 8 (UUO surgery); **P* < 0.01 vs. sham surgery; $^{\#}P$ < 0.01 vs. UUO treated with vehicle (ANOVA with Bonferroni's multiple comparison test).

A

Donor	Age	Sex	Basic Pathology	Procedure Type
1	64	M	Diabetic Nephropathy	Surgical
2	55	M	Diabetic Nephropathy	Biopsy
3	42	F	Diabetic Nephropathy	Biopsy
4	62	F	Diabetic Nephropathy	Surgical
5	47	F	Diabetic Nephropathy	Biopsy
6	47	M	Diabetic Nephropathy	Biopsy
7	58	F	Diabetic Nephropathy	Biopsy
8	44	M	Diabetic Nephropathy	Surgical
9	44	F	Diabetic Nephropathy	Surgical
10	31	F	Diabetic Nephropathy	Surgical

B

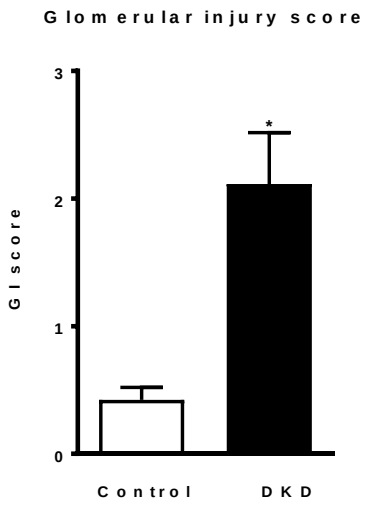

C

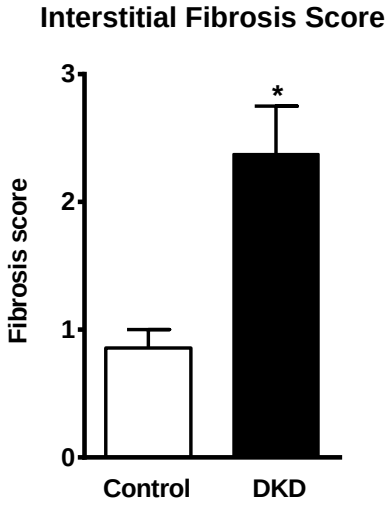

Supplementary Figure 11. **Characteristics of biopsies from DKD patients. (A)** Formalin-fixed, paraffin-embedded renal biopsy tissues from patients with diabetic kidney disease (DKD) (n = 10) and healthy controls (n = 7) were commercially sourced (Folio Biosciences, LLC). Semi-quantification of (**B**) glomerular injury score (0-4) was assessed on periodic acid–Schiff-stained sections and (**C**) interstitial fibrosis score (0-4) was assessed on Masson's trichrome-stained sections by a board-certified renal pathologist according to established criteria (1). Data are mean ± SEM; **P* < 0.05 (unpaired *t* test).

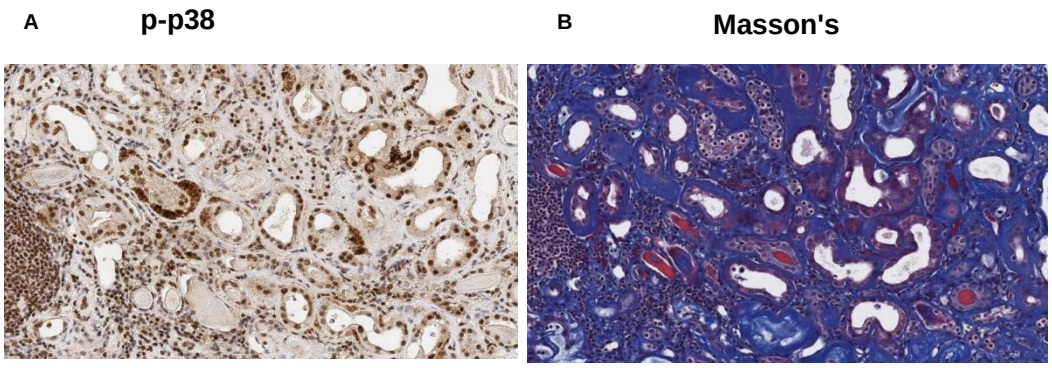

Supplementary Figure 12. **p-p38 immunostaining is prominent in areas of tubulointerstitial fibrosis in kidneys from DKD patients.** Formalin-fixed, paraffin-embedded renal biopsy tissues from patients with diabetic kidney disease (DKD) (n = 10) were commercially sourced (Folio Biosciences, LLC). Representative serial sections of a DKD kidney biopsy (**A**) immunostained for p-p38 or (**B**) stained with Masson's trichrome.

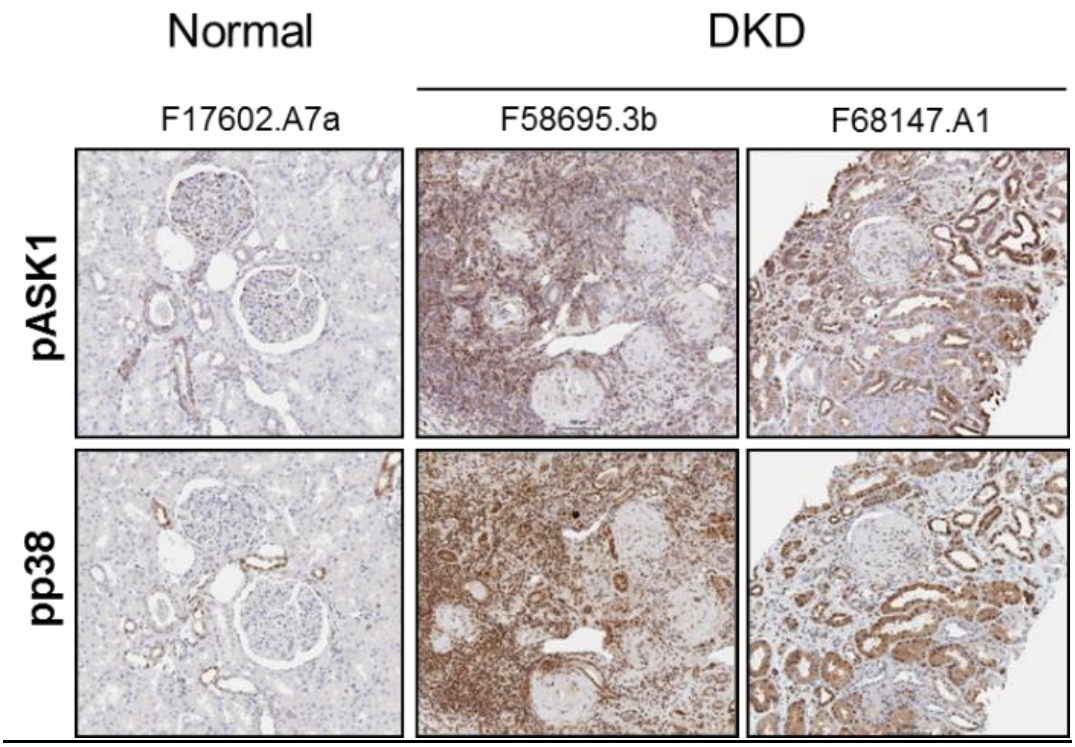

Supplementary Figure 13. **Representative images of p-ASK1 and p-p38 immunostaining in serial sections from renal biopsies from normal and DKD patients.** Activation of the ASK1 pathway was evaluated in renal biopsies using a newly developed antibody that specifically recognizes the autophosphorylated active form of ASK1 (ASK1 T845; p-ASK1) and with an antibody that recognizes the activated phosphorylated form of p38 (p-p38). Representative immunostaining for p-ASK1 and p-p38 in serial sections from normal kidneys (F17602.A7a) and kidneys from patients with diabetic kidney disease (DKD; F58695.3b; F68147.A1). Glomerular (top panels) and tubulointerstitial compartments (bottom panels) are shown. Similar cell types and distribution within compartments were noted for both antibodies. Formalin-fixed, paraffin-embedded renal biopsy tissues were commercially sourced (Folio Biosciences, LLC).

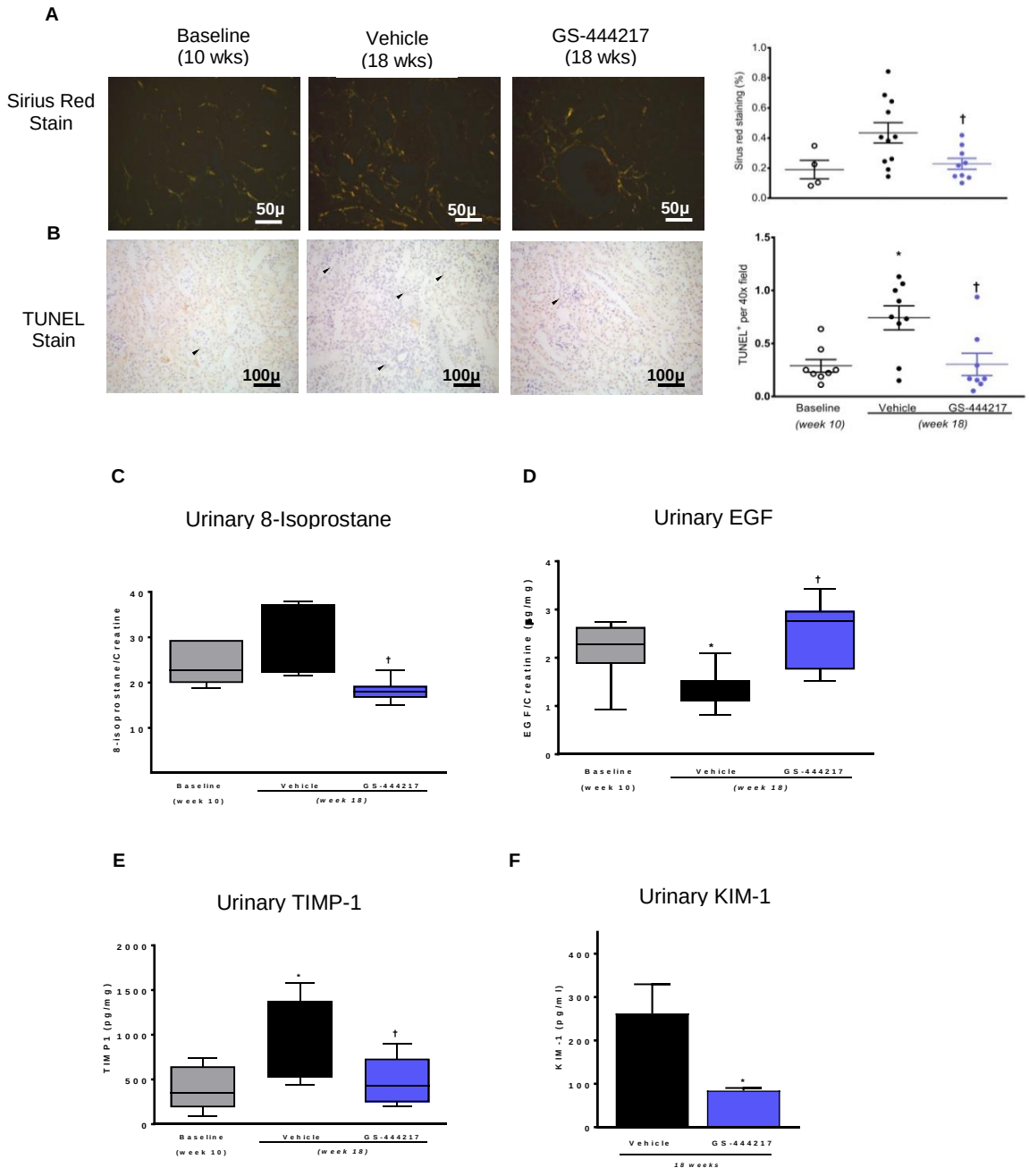

Supplementary Figure 14. **GS-444217 regulated urinary biomarkers related to kidney injury, function, and fibrosis in a mouse model of diabetic kidney disease**. (**A-F**) 10-week-old db/db eNOS$^{-/-}$ mice were fed standard rodent chow (vehicle) or chow containing GS-444217 (0.3% by weight) for 8 weeks. A separate group of untreated db/db eNOS$^{-/-}$ mice were euthanized at 10-weeks-of-age to establish baseline disease parameters. At 18 weeks, Image analysis and graphed pathology scores of renal sections stained for (**A**) interstitial fibrosis (Sirius red), and (**B**) interstitial apoptosis (TUNEL stain) were performed. At 18 weeks, urinary concentrations of (**C**) 8-isoprostane [n = 6 (baseline), n = 5 (vehicle) n = 6 (GS-444217)], (**D**) epidermal growth factor [EGF; n = 6 (baseline), n = 10 (vehicle) n = 9 (GS-444217)] (**E**) tissue inhibitor of metalloproteinase-1 [TIMP-1; n = 5 (baseline), n = 8 (vehicle) n = 7 (GS-444217)], and (**F**) kidney injury molecule-1 [KIM-1; n = 13 (vehicle) n = 10 (GS-444217) were measured in urine. Scale bars = 100 µm (**A**) 50 µm (**B**). Data in **C-F** are mean ± SEM; **P* < 0.05 vs. 10-week baseline (unpaired *t* test), †*P* < 0.05 vs. vehicle (ANOVA with Bonferroni's multiple comparison test).

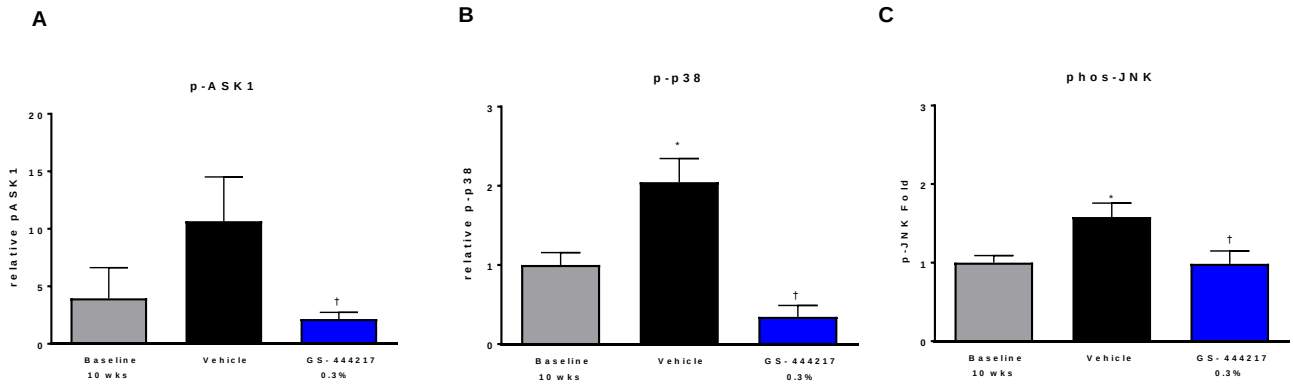

Supplementary Figure 15. **GS-444217 decreases ASK1 pathway activation in kidneys db/db eNOS$^{-/-}$ mice.** 10-week-old db/db eNOS$^{-/-}$ mice were fed standard rodent chow (vehicle) or chow containing GS-444217 (0.3% by weight) for 8 weeks. A separate group of untreated db/db eNOS$^{-/-}$ mice were euthanized at 10-weeks-of-age to establish baseline disease parameters. After 8 weeks of treatment, renal cortex was collected when plasma levels of GS-444217 were near peak levels. Western blot signals were quantified for (**A**) p-ASK1, (**B**) p-p38, and (**C**) p-JNK. Data are mean ± SEM, n = 7 (10-week baseline), n = 11 (18 week), n = 7 (GS-444217); *$P < 0.05$ vs. 10-week baseline; †$P < 0.05$ vs. 18 weeks (ANOVA with Newman-Keuls multiple comparison test).

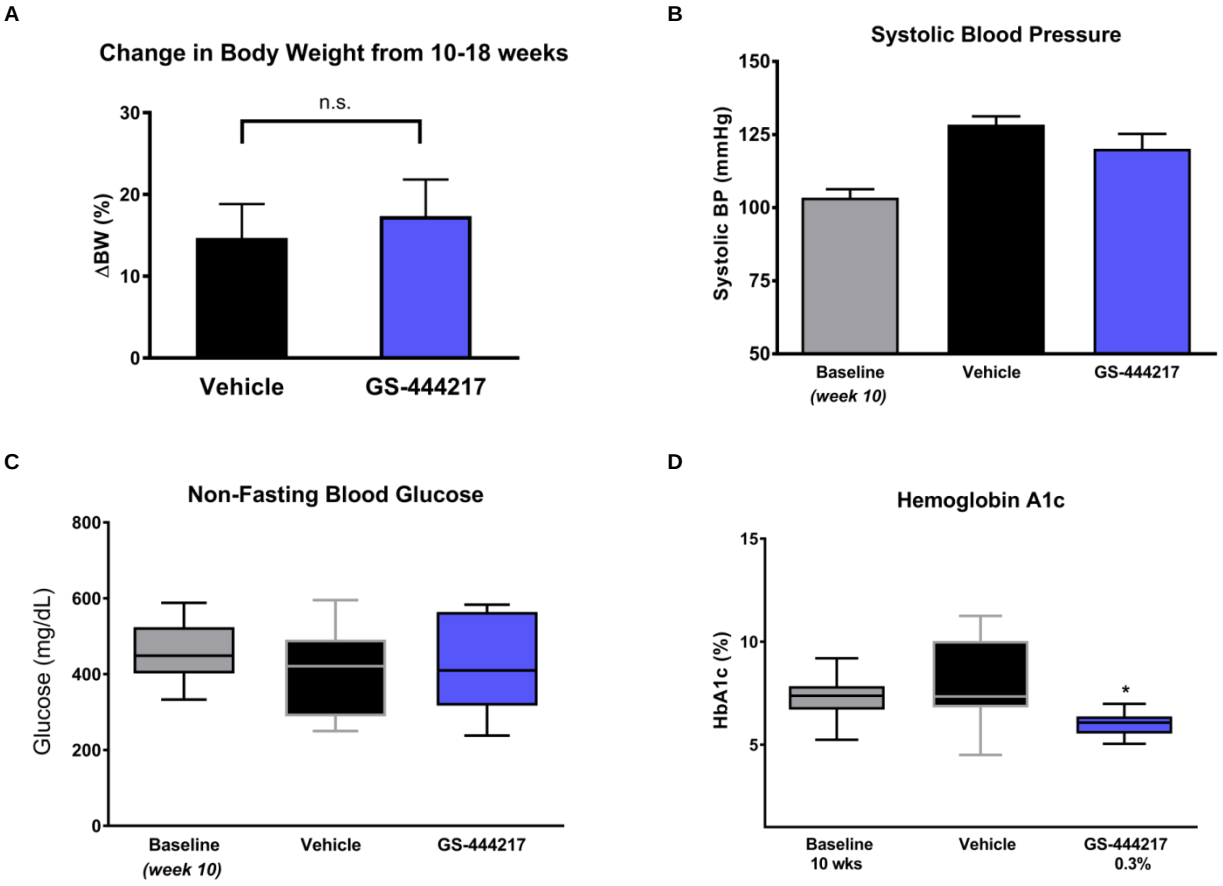

Supplementary Figure 16. **Treatment with GS-444217 did not alter body weight, blood pressure, or blood glucose in db/db eNOS$^{-/-}$ mice.** 10-week-old db/db eNOS$^{-/-}$ mice were fed standard rodent chow (vehicle) or chow containing GS-444217 (0.3% by weight) for 8 weeks. A separate group of untreated db/db eNOS$^{-/-}$ mice were euthanized at 10-weeks-of-age to establish baseline disease parameters. Comparisons of (**A**) change in weight (ΔBW) from 10 weeks to 18 weeks [n = 16 (vehicle) n = 9 (GS-444217)]; (**B**) systolic blood pressure (BP) measured by tail cuff [n = 7 (baseline), n = 13 (vehicle) n = 6 (GS-444217)]; (**C**) non-fasting blood glucose concentrations [n = 8 (baseline), n = 14 (vehicle) n = 9 (GS-444217)]; (**D**) percent hemoglobin A1c (HBA1c) [n = 15 (baseline), n = 12 (vehicle) n = 8 (GS-444217)]. Glucose and HbA1c were measured with a clinical chemistry analyzer. Data are mean ± SEM; *P < 0.05 (ANOVA with Newman-Keuls multiple comparison test).

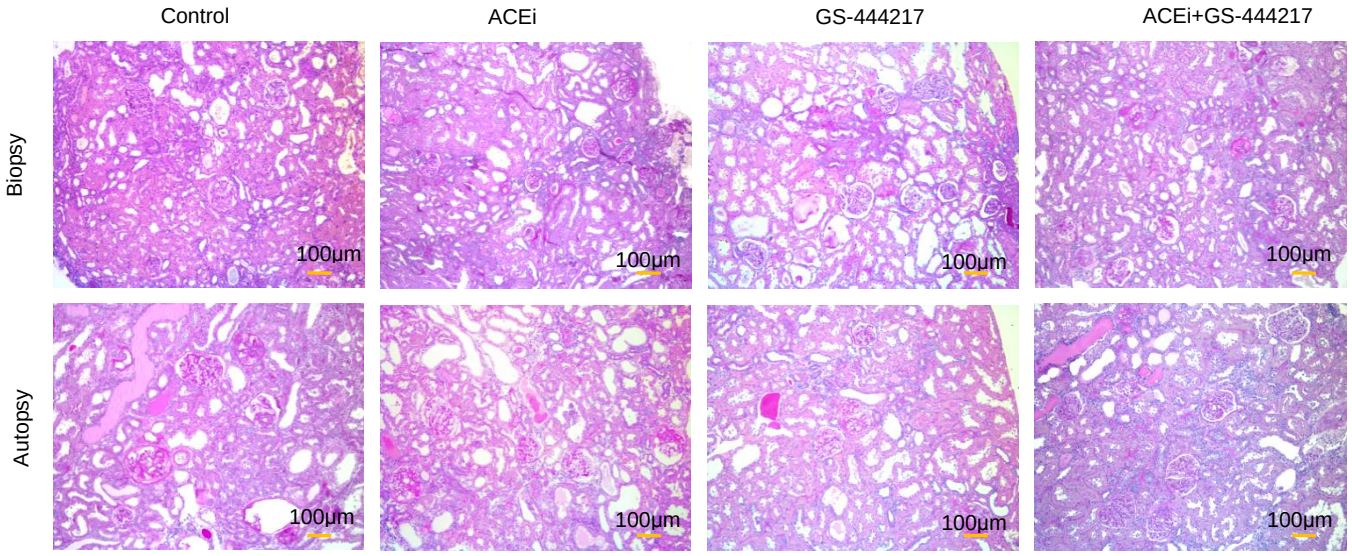

Supplementary Figure 17. **Representative images of PAS-stained kidney sections at biopsy and autopsy from 5/6th Nephrectomy experiments.** Scale bars = 100 µm

Supplementary Tables

Table 1. ADME Parameters for GS-444217

ADME Parameters for GS-444217	
Solubility (pH 7.4)	41.6 µg/mL
CACO AB / BA	8 / 66 (10^{-6} cm/s)
Predicted clearance (rat, human)	0.67, 0.26 L/hr/kg

Absorption, distribution, metabolism, and excretion (ADME) parameters for GS-444217 showing solubility, permeability (apical to basolateral (A-B) and basolateral to apical (B-A) in Caco-2 cells), and predicted clearance in rat and human.

Table 2. Pharmacokinetic Parameters of GS-444217 in Rats Following Oral Administration

	10 mg/kg, p.o. **Mean ± SD**	**30 mg/kg, p.o.** **Mean ± SD**
AUC_{last} (nM·hr)	100,207 ± 35,996	365,622 ± 45,458
C_{max} (nM)	25,234 ± 6,462	65,546 ± 10,239
$t_{1/2}$ (hr)	2.07 ± 0.05	2.84 ± 0.98
F (%)	89.6	109

GS-444217 plasma concentrations were measured by HPLC coupled to tandem mass spectrometry following a single oral gavage of 10 or 30 mg/kg to non-fasted Sprague-Dawley rats (mean ± SD, n = 3 per group), and pharmacokinetic parameters were determined for: AUC_{last} (area under the curve up to the last measurable concentration); C_{max} (maximum plasma concentration); $t_{1/2}$ (time required for the concentration to fall to half of its original value); F (fraction of bioavailability).

Supplementary Methods

Pharmacokinetic analytical methods

Supplementary Figure 2: Concentrations of GS-444217 in plasma samples were measured using standard methods for HPLC coupled to tandem mass spectrometry (LC/MS/MS). These methods were developed for selectivity, sensitivity, linearity, intra-assay accuracy, and precision. GS-444217 was formulate in rodent chow as described in the main methods.

In vitro oxidative stress-induced activation and inhibition of endogenous ASK1

Supplementary Figure 3: Neonatal rat ventricular myocytes were treated with 1 µM GS-44421720 or medium for 1 hour before addition of 20 µM auranofin (thioredoxin reductase inhibitor) or 10 µM 2-acetylamino-3-[4-(2-acetylamino-2-carboxyethylsulfanylthiocarbonylamino) phenylthiocarbamoylsulfanyl] propionic acid (2-AAPA, glutathione reductase inhibitor) for 0 to 60 minutes, or with 20 µM diethyldithiocarbamate (DDC, superoxide dismutase inhibitor) for 0 to 300 minutes. HK-2 immortalized proximal tubule epithelial cells were pretreated with GS-444217 (0, 0.1, 1 µM) followed by treatment with 1 µM H_2O_2 for 5 min. At the end of the incubation period, cells were washed in ice cold polybuffered saline, lysed in ice cold RIPA buffer with HALT Protease inhibitor cocktail, and immediately frozen on dry ice. Protein lysates were quantified by BCA Reagent (18611426, Pierce) and Western blot analysis was performed. The following antibodies were used to probe the blots (all at dilutions of 1:1000): phosphorylated ASK1-T_{845} (3765S, Cell Signaling), phosphorylated p38-T_{180}/Y_{182} (9211S, Cell Signaling), β-tubulin (2128, Cell Signaling), or IP-90 (sc-11397, Santa Cruz). Femto chemiluminescent substrate (34096, Thermo Fisher scientific) was used for signal detection.

Auranofin in vivo pharmacodynamic model: proof-of-concept

Supplementary Figure 5A-E: Sprague-Dawley rats were administered auranofin (10 and 30 mg/kg, intraperitoneal (i.p.), n = 8) or vehicle (equal volume, i.p., n = 8) and renal cortex lysates were analyzed 30 min later for p-ASK1, p-p38, and p-JNK by Western blotting as described in main methods for "auranofin in vivo pharmacodynamic model", IL-1β mRNA expression by real-time RT-PCR, and caspase-3 activity by according to manufacturer's instructions (Thermo Fisher Scientific).

Rat renal ischemia and reperfusion (I/R) injury model

The model and experimental methods are described in the main methods. **Supplementary Figures 7 and 8**: Sections from the right kidneys were stained with H&E, for caspase-3 activity, and for apoptosis with TUNEL. The left kidney was snap-frozen in liquid nitrogen, mRNA extracted, and Luminex performed for *Ccl2*, *Cxcl2*, *Cxcl1*, *Il1b*, *Il6*, *Il2*, *Il10*, *Tnfa*, and *Tgfb1* expression. Expression values were normalized to *Hprt* housekeeping gene.

Rat unilateral uretal obstruction (UUO) model

The model and experimental methods are described in the main methods. **Supplementary Figures 9 and 10**: The left kidney was snap-frozen in liquid nitrogen, mRNA extracted, and real-time RT-PCR performed for collagen IV (*Col4a1*), *Tgfb1*, alpha-smooth muscle actin (*Acta1*), connective tissue growth factor (*Ctgf*), plasminogen activator inhibitor-1 (*Serpine1*). Expression values were normalized to 18S rRNA.

p-p38 immunohistochemistry in human renal biopsies

Supplementary Figures 11 and 12: Formalin-fixed paraffin-embedded renal biopsy tissues from 10 patients with DKD and from 7 control subjects without kidney disease ("healthy") were obtained from Folio Biosciences. Sections were immunostained for p-p38 using a rabbit p38 MAPK mAb (9212S, Cell Signaling). Whole-slide images were quantified using Tissue Studio® software (Definiens) and expressed as a cellular H-score, which quantifies stain intensity and distribution. Semi-quantification of glomerular injury score (0-4) was assessed on periodic acid–Schiff-stained sections and interstitial fibrosis score (0-4) was assessed on Masson's trichrome-stained sections by a board-certified renal pathologist according to established criteria (1).

p-ASK1 and p-p38 immunohistochemistry in human renal biopsies

Supplementary Figure 13: Formalin-fixed paraffin-embedded renal biopsy tissues from 2 patients with DKD and from a control subject without kidney disease ("normal") were obtained from Folio Biosciences. Serial sections were immunostained using an antibody that specifically recognizes the ASK1 T845 autophosphorylated active form (p-ASK1) and with an antibody that recognizes the activated phosphorylated form of p38 (p-p38; 9212S, Cell Signaling). The p-ASK antibody was generated by immunizing rabbits with the catalytic domain of human ASK1 (verified by mass spectroscopy to be phosphorylated at a single site, Thr-838). Rabbit sera were assessed by ELISA to detect phosphorylated vs. total ASK1 and positive rabbit spleens were then fused to generate hybridoma monoclonal antibodies. Positive hybridoma clones were then sequenced and antibodies validated as being p-ASK specific by ELISA, IHC, and Western blot. Antibody phospho-specificity was further assessed by loss of IHC signal on formalin immersed tissues treated with phosphatase.

db/db eNOS$^{-/-}$ mouse model of DKD

The model and experimental methods are described in the main methods. **Supplementary Figure 14**: 8-isoprostane in urine was measured with an EIA kit (Oxford Biomedical Research). Urinary epidermal growth factor (EGF), metallopeptidase inhibitor-1 (TIMP-1), kidney inury molecule-1 (KIM-1) were measure by ELISA (R&D Systems) and normalized to urine creatinine levels determined using an enzymatic mouse creatinine assay kit (80350, Crystal Chem).

Supplementary Figure 15A-C: *Western blot:* Renal cortex lysates were obtained and 25 µg protein samples were prepared for Western blotting as described in main methods for "auranofin in vivo

pharmacodynamic model" samples. Primary antibodies (rabbit polyclonal phosphorylated Th838-ASK1 (Gilead Sciences, Inc.), phosphorylated-p38 (9211S, Cell Signaling), phosphorylated-JNK (9251S, Cell Signaling), IP-90 (sc-11397, Santa Cruz Biotechnology) were used at 1:1000 dilutions and the secondary anti-rabbit HRP-linked antibody was used at 1:2000 dilution.

Supplementary Figure 16B: *Blood pressure:* Systolic blood pressure was measured in conscious mice prior to sacrifice using tail-cuff impedance plethysmography (BP-2000 Blood Pressure Analysis System, Visitech Systems). Mice were acclimated to the procedure. Mean values were based on an average of 10 stable readings.

Supplementary Figure 16C,D: Percent hemoglobin A1c (HbA1c) and non-fasting blood glucose were analyzed in plasma with an Olympus AU400 clinical chemistry instrument (Beckman Coulter, Inc.).

Supplementary References

1. Tervaert TW, Mooyaart AL, Amann K, et al. Pathologic classification of diabetic nephropathy. *J Am Soc Nephrol.* 2010;21(4):556–563.

Supplemental Note on Chemical Synthesis

General Information. All air or moisture sensitive reactions were conducted under a dry nitrogen atmosphere. The first reagent shown in each scheme was available from a commercial source. Solvents and other reagents were obtained from VWR or Aldrich and were used without any additional purification. H NMR spectra were recorded at 400 MHz using a Varian instrument.

N-(3-(4-methyl-4H-1,2,4-triazol-3-yl)phenyl)picolinamide (1):

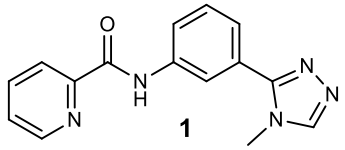

1

(CAS# = 1147769-55-8) is commercially available from several vendors including Enamine (Order Number: Z364883930).
^{1}H NMR (400 MHz, CD_3OD) δ 8.72 (dd, J = 0.8, 4.8 Hz, 1H), 8.57 (s, 1H), 8.25 (t, J = 1.2 Hz, 1H), 8.22 (d, J = 8.0 Hz, 1H), 7.98-8.04 (m, 2H), 7.57-7.63 (m, 2H), 7.52 (d, J = 8.0 Hz, 1H), 3.86 (s, 3H). ^{13}C NMR (100 MHz, CD_3OD) δ 163.41, 149.53, 148.33, 138.60, 137.66, 129.40, 126.72, 126.53, 124.36, 122.10, 122.00, 120.18, 31.52.
HRMS (ESI+) *m/z* calc'd for $C_{15}H_{13}N_5O$ $[M+H]^+$: 279.1120, found 279.1121.

3-(4-cyclopropyl-4H-1,2,4-triazol-3-yl)aniline (common intermediate **6**):

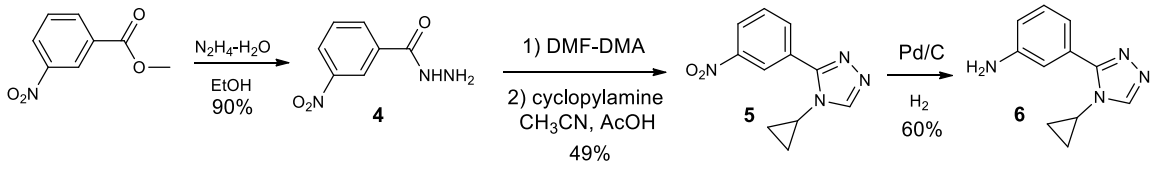

Step 1: 3-nitrobenzohydrazide (**4**)
To a solution of methyl 3-nitrobenzoate (660 g, 1220 mmol) in EtOH (4 L), hydrazine hydrate (960 mL, 18.27 mol) was added. The resulting mixture was stirred at reflux for 2.5 hr and cooled to room temperature. The solvent was removed by concentration in vacuo and the residue solid was washed with ether to give 3-nitrobenzohydrazide (**4**) as a white solid (600 g, 90% yield).
^{1}HNMR (400 MHz, DMSO-d6): δ 10.15 (s, 1 H), 8.64 (t, J = 2.0 Hz, 1 H), 8.35-8.38 (m, 1 H), 8.24-8.26 (m, 1 H), 7.79 (t, J = 8.0 Hz, 1 H), 4.61 (s, 2 H). LC-MS (ESI+) m/z calc'd for $C_7H_7N_3O_3$ $[M+H]^+$: 182, found 182.

Step 2: 4-cyclopropyl-3-(3-nitrophenyl)-4H-1,2,4-triazole (**5**)
A solution of **4** (479 g, 2.65 mol) in DMF-DMA (3.2 kg) was stirred at 50 °C for 50 min and then cooled to room temperature. The precipitate formed in the mixture was collected by filtration and dissolved in CH_3CN (1500 mL). To this solution, cyclopropylamine (755 g, 13.2 mol) and AcOH (1000 mL) were added. The resulting mixture was heated to 120 °C for 15 hr and then cooled to room temperature, concentrated in vacuo to remove

the volatile solvent. The residue was diluted with water and extracted with DCM (3 x 1L). The combined organic layers were washed with saturated Na_2CO_3 (aq) and brine, and dried over anhydrous Na_2SO_4. The solvents were removed by concentration in vacuo. The residue was recrystallized from DCM and PE to give 4-cyclopropyl-3-(3-nitrophenyl)-4H-1,2,4-triazole (**5**) as a white solid (300 g, 49% yield).
^{1}HNMR (400 MHz, CDCl3): δ8.84 (t, J = 1.6 Hz, 1 H), 8.37 (q, J = 1.6 Hz, 2 H), 8.28 (s, 1 H), 7.74 (t, J = 8.4 Hz, 1 H), 3.50-3.55 (m, 1 H), 1.22-1.27 (m, 2 H), 0.96-1.00 (m, 2 H). LC-MS (ESI+) m/z calc'd for $C_{11}H_{10}N_4O_2$ $[M+H]^+$: 231, found 231.

Step 3: 3-(4-cyclopropyl-4H-1,2,4-triazol-3-yl)aniline (**6**)
To a mixture of **5** (300 g, 1.3 mol) and Pd/C (60 g) in MeOH (3 L) was stirred at room temperature under H_2 atmosphere for 72 hr. The catalyst was removed by filtration through a short celite pad. The filtrate was concentrated in vacuo and the residue obtained was recrystallized from DCM to give 3-(4-cyclopropyl-4H-1,2,4-triazol-3-yl)aniline (**6** as a white solid (156 g, 60% yield).
^{1}H NMR (400 MHz, DMSO-d6): δ 8.53 (s, 1H), 7.15 (t, J = 7.6 Hz, 1H), 7.09 (d, J = 1.6 Hz, 1H), 7.02 (d, J = 7.6 Hz, 1H), 6.69 (m, 1H), 5.30 (s, 2H), 3.53 (m, 1H), 0.88-1.04 (m, 4H). LC-MS (ESI+) m/z calc'd for $C_{11}H_{12}N_4$ $[M+H]^+$: 201, found 201.

N-(3-(4-cyclopropyl-4H-1,2,4-triazol-3-yl)phenyl)-[3,4'-bipyridine]-2'-carboxamide (2):

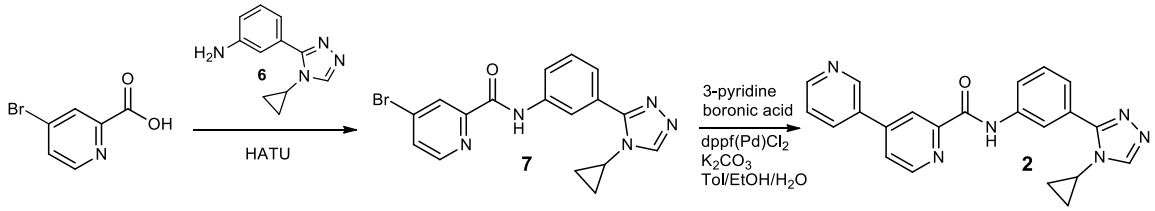

To a solution of 4-bromopicolinic acid (5.76 g 28.5 mmol), 3-(4-cyclopropyl-4H-1,2,4-triazol-3-yl)aniline (**6**) (5.70 g, 28.5 mmol), and HATU (10.9 g, 28.7 mmol) in DMF (28.5 mL) was added N,N-diisopropylethylamine (10.0 mL, 61.2 mmol) and the reaction was stirred at room temperature for 15 minutes. The solvent was removed under vacuum and the residue was suspended in acetonitrile (100 mL) and water (100 mL) and the solid was isolated by filtration and washed with ether to afford 4-bromo-N-(3-(4-cyclopropyl-4H-1,2,4-triazol-3-yl)phenyl)picolinamide (**7**) as a white powder (7.4 g, 68% yield) which was used directly in the subsequent reaction. LC-MS (ESI+) m/z calc'd for $C_{17}H_{14}BrN_5O$ $[M+H]^+$: 384, found 384.
A suspension 4-bromo-N-(3-(4-cyclopropyl-4H-1,2,4-triazol-3-yl)phenyl)picolinamide (**7**) (120 mg, 0.31 mmol), 3-pyridine boronic acid (77 mg, 0.62 mmol), dppf(Pd)Cl_2 (23 mg, 0.03 mmol), and potassium carbonate (86 mg, 0.62 mmol) in degassed toluene (2 mL), degassed water (1 mL) and degassed ethanol (1 mL) was heated at 100°C for 1 hour. The solvent was removed and the residue was purified by reverse-phase HPLC to give [3,4']bipyridinyl-2'-carboxylic acid [3-(4-cyclopropyl-4H-[1,2,4]triazol-3-yl)-phenyl]-amide (**2**) as a white solid (58 mg, 48% yield).
^{1}H NMR (DMSO-d6) δ 10.98 (s, 1H), 9.12 (d, J = 1.6 Hz, 1H), 8.87 (d, J = 4.8 Hz, 1H), 8.72 (dd, J = 1.2, 4.8 Hz, 1H), 8.63 (s, 1H), 8.60 (s, 1H), 8.48 (d, J = 1.2 Hz, 1H), 8.34 (m, 1H), 8.11 (m, 2H), 7.69 (d, J = 8.0 Hz, 1H), 7.59 (m, 2H), 3.66 (m, 1H), 1.09 (m,

2H), 0.94 (m, 2H). ^{13}C NMR (100 MHz, DMSO-d6) δ 163.13, 154.08, 151.28, 151.03, 149.79, 148.45, 146.77, 146.01, 139.09, 135.26, 132.74, 129.52, 128.21, 124.89, 124.64, 124.17. 121.94, 120.39, 120.29, 27.50, 8.07.
HRMS (ESI+) *m/z* calc'd for $C_{22}H_{18}N_6O$ $[M+H]^+$: 382.1542, found 382.1553.

4-(4-cyclopropyl-1H-imidazol-1-yl)-N-(3-(4-cyclopropyl-4H-1,2,4-triazol-3-yl)phenyl)picolinamide (3):

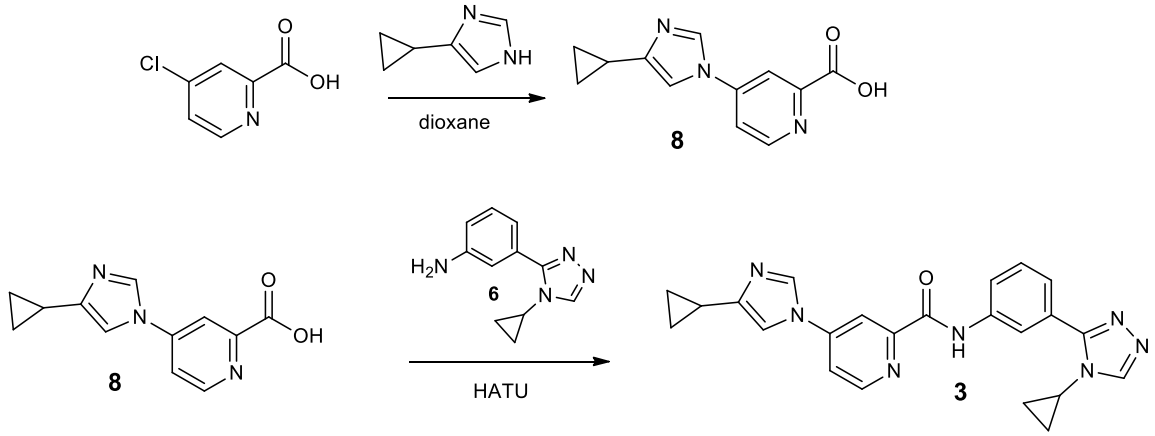

Step 1: 4-(4-cyclopropyl-1H-imidazol-1-yl)picolinic acid (**8**):
4-Chloropyridine-2-carboxylic acid (483 g, 3.1 mol), 4-cyclopropyl-1H-imidazole (1000 g, 9.12 mol) and 1, 4-dioxane (15 L) were stirred at reflux for 44 hours. Volatiles were removed under vacuum, and the residue was dissolved in a solution of NaOH (246 g, 6.17mol) in water (3000 ml), adjusted to pH>14, and extracted with DCM (8 x 2 L). The aqueous layer was acidified to pH=4, solids precipitated and were filtered to afford a white solid, which was stirred in MeOH (17 L) at reflux, filtered to remove insoluble material, and the filtrate was concentrated to a volume of 1L, filtered and the solids were washed with MeOH and water to afford 4-(4-cyclopropyl-1H-imidazol-1-yl)picolinic acid (**8**) as an off-white solid (342 g, 48% yield).
^{1}H NMR (D_2O) δ 8.91 (s, 1H), 8.68 (d, J = 5.2 Hz, 1H), 8.13 (s, 1H), 7.79 (m, 1H), 7.61 (s, 1H), 1.89-1.94 (m, 1H), 0.94-0.99 (m, 2H), 0.70-0.75 (m, 2H). LC-MS (ESI+) m/z calc'd for $C_{12}H_{11}N_3O_2$ $[M+H]^+$: 230.1, found 230.2.

Step 2: 4-(4-cyclopropyl-1H-imidazol-1-yl)-N-(3-(4-cyclopropyl-4H-1,2,4-triazol-3-yl)phenyl)picolinamide (**3**):
To a mixture of 4-(4-cyclopropyl-1H-imidazol-1-yl)picolinic acid (**8**) (50 g, 216 mmol), EDCI (53.8 g, 281 mmol) and HOBT (35 g, 259 mmol) in DMF (100 mL) at 10 °C was added 3-(4-cyclopropyl-4H-1,2,4-triazol-3-yl)aniline (**6**) (45.4 g, 227 mmol) and N-methyl morpoline (31 mL, 281 mmol) was added dropwise. The reaction mixture was warmed to room temperature, stirred for 48 hr and then diluted with NaOH (400 mL, 0.1N). The resulting mixture was stirred at 10 °C for 1 hour and filtered. The solid was washed with i-PrOH and Et_2O, and dried in vacuo to afford 4-(4-cyclopropyl-1H-imidazol-1-yl)-N-(3-(4-cyclopropyl-4H-1,2,4-triazol-3-yl)phenyl)picolinamide (**3**) (61 g, 69% yield).
^{1}H NMR (400 MHz, $CDCl_3$) δ 10.94 (s, 1 H), 8.79 (d, J = 5.2 Hz, 1 H), 8.63 (s, 1 H), 8.58 (m, 2 H), 8.37 (d, J = 2.0 Hz, 1 H), 8.07 (d, J = 8.0 Hz, 1 H), 7.99 (dd, J = 2.4, 5.6 Hz, 1 H), 7.86 (d, J = 1.2 Hz, 1 H), 7.70 (d, J = 7.6 Hz, 1 H), 7.57 (t, J = 8.0 Hz, 1 H),

3.68 (m, 1 H), 1.88 (m, 1 H), 1.09 (m, 2 H), 0.96 (m, 2 H), 0.86 (m, 2 H), 0.75 (m, 2 H).
^{13}C NMR (100 MHz, DMSO-d6) δ 162.71, 154.04, 152.52, 150.70, 146.34, 146.01, 145.10, 138.99, 135.69, 129.52, 128.21, 124.23, 121.94, 120.27, 116.35, 112.24, 112.19, 27.50, 9.35, 8.09, 7.49.
HRMS (ESI+) *m/z* calc'd for $C_{23}H_{21}N_7O$ $[M+H]^+$: 411.1808, found 411.1817.

Figure S1

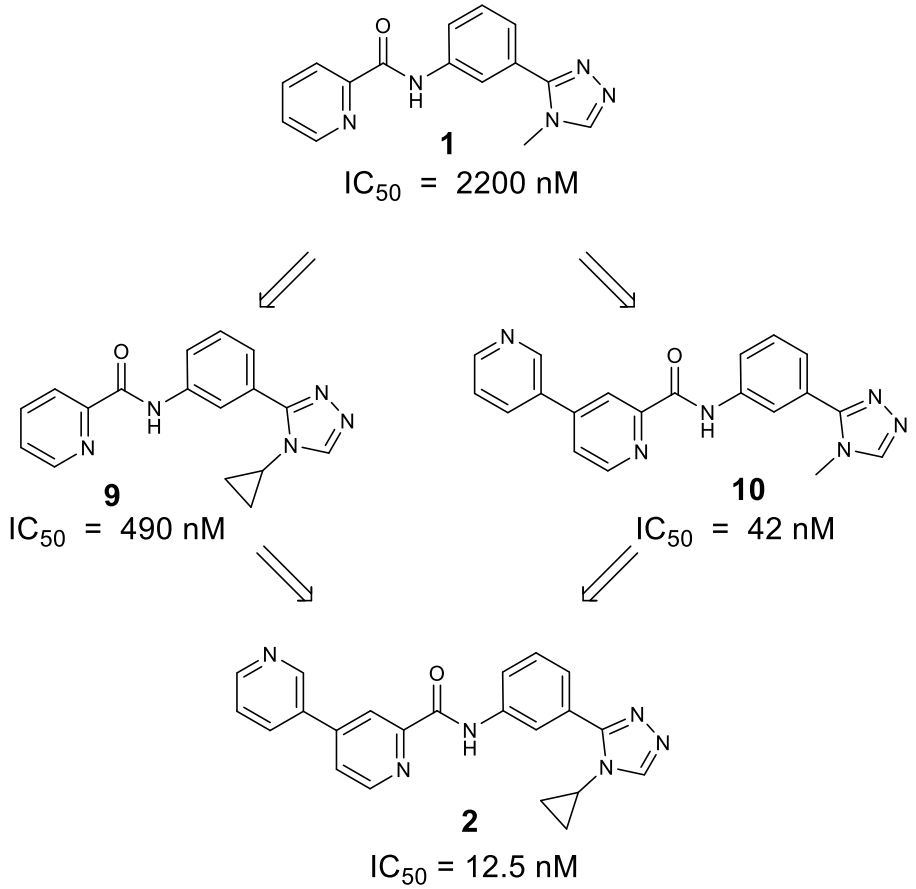

Figure S1. Potency and structure of compounds **9** and **10**, and additive nature of these changes when combined to provide compound **2**

^{1}H NMR spectra for compounds **1-3:**

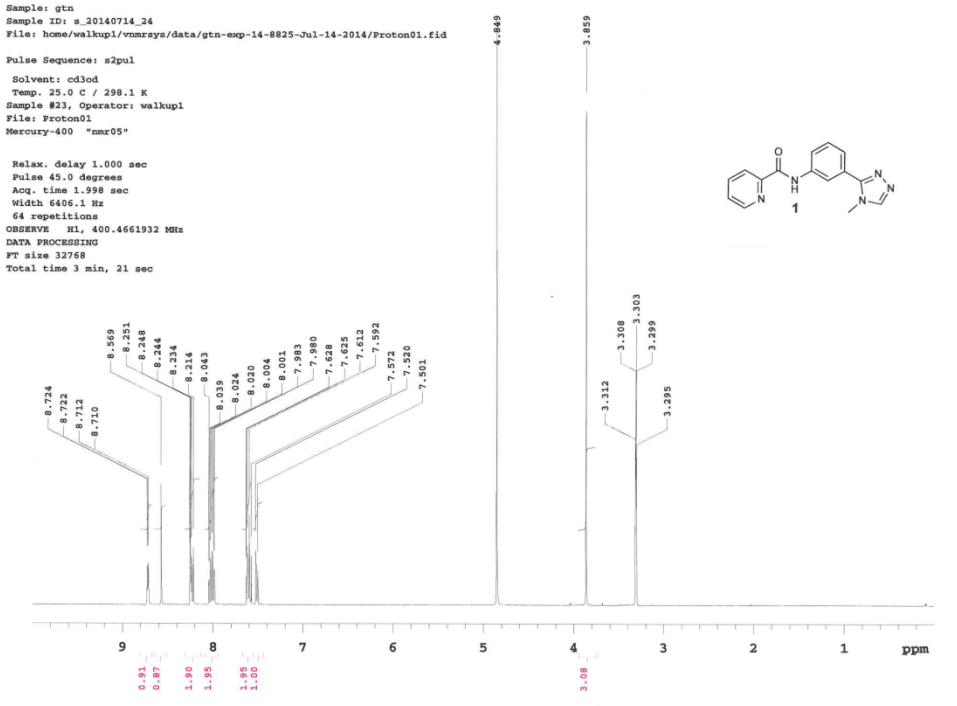

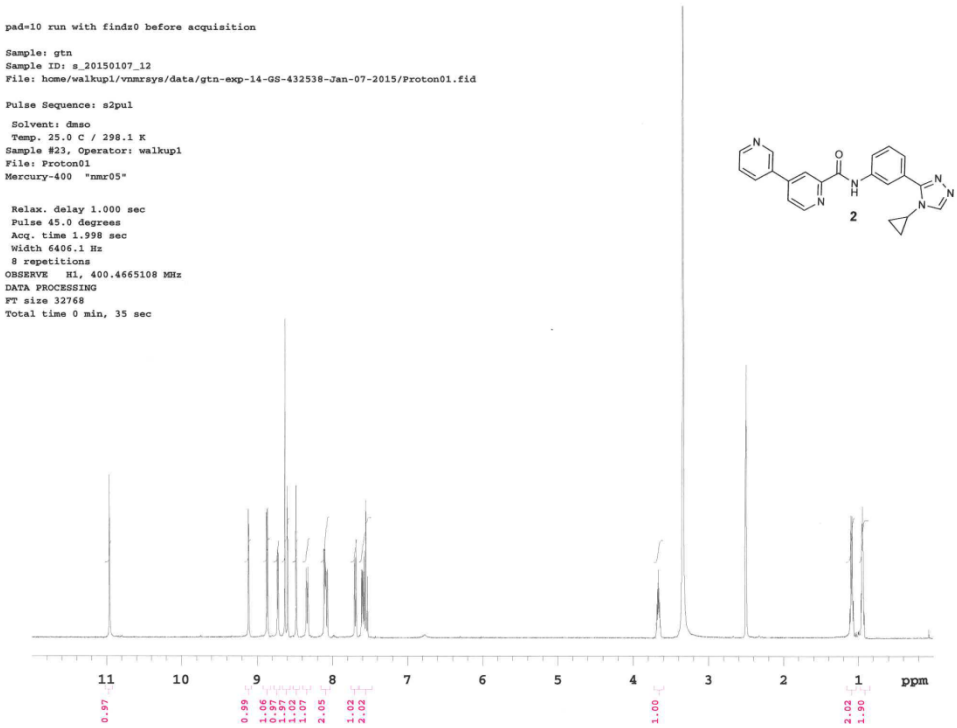

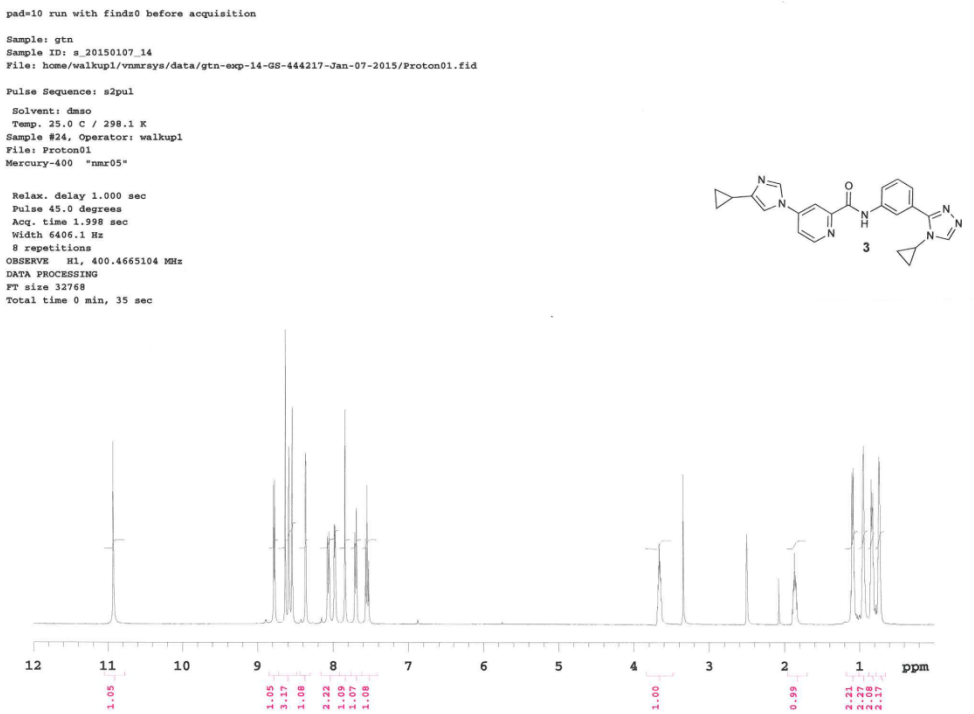

Crystallization Studies

Crystals of ASK1 kinase domain (residues 659-951) were grown by hanging drop vapor diffusion over a mother liquor containing 25% PEG 400, 3% PPG P 400, 100 mM Bis-Tris pH 7.5, and 10mM TCEP at 20°C. Equal parts of protein and reservoir solution were mixed. Crystals were moved to a solution containing 30% PEG 400, 100mM Bis-Tris pH 7.5, 10 mM TCEP and 0.5 mM GS-4997 for 6 hours prior to data collection and then cryocooled in liquid nitrogen. Data was collected at a temperature of 100K at The Advanced Light Source and processed with HKL2000 (1). Molecular replacement of the ASK1 kinase was performed with the refinement software package Phenix (2) using the starting model PDB code 2CLQ. Rigid body refinement, simulated annealing, energy minimization, and B-factor refinement were likewise carried out with Phenix. Bulk solvent correction and anisotropic B-factor scaling were used during refinement. Model building was performed with the molecular graphics program Coot (3).

Competitive, time-resolved fluorescence resonance energy transfer (TR-FRET) assay

Experiment performed based on HTRF® KinEASE™-STK manual from Cisbio. GS-444217, 1 μM STK3 peptide substrate, 4 nM of ASK1 kinase was incubated with 10 mM MOP buffer, pH. 7.0 containing 10 mM Mg-acetate, 0.025 % NP-40, 1 mM DTT, 0.05% BSA and 1.5% glycerol for 30 minutes then 100 μM ATP is added to start the kinase reaction and incubated for 3 hr. Peptide antibody labeled with 1X Eu^{3+} cryptate buffer

containing 10 mM EDTA and 125 nM streptavidin XL665 was added to stop the reaction, and phosphorylated peptide substrate was detected using Envision 2103 Multilabel plate reader from PerkinElmer. The fluorescence was measured at 615 nm (cryptate) and 665 nm (XL665) and a ratio of 665 nm/615 nm was calculated for each well. The resulting TR-FRET level (a ratio of 665 nm/615 nm) is proportional to the phosphorylation level. Under these assay conditions, the degree of phosphorylation of peptide substrate was linear with time and concentration for the enzyme. The assay system yielded consistent results with regard to K_m and specific activities for the enzyme.

For inhibition experiments (IC_{50} values), activities were performed with constant concentrations of ATP, peptide and several fixed concentrations of inhibitors. Staurosporine, the nonselective kinase inhibitor, was used as the positive control. All enzyme activity data were reported as an average of quadruplicate determination.

Enzymological Assays with ATP

A stock solution of 17 μM dephosphorylated ASK1 protein was pre-incubated with 200 μM ATP for 10 min at room temperature to activate the protein. The activated enzyme was subsequently diluted to the final concentrations used in the assays. For the ATP competition study of GS-444217, GS-444217 at various concentrations from 0-24 nM and ATP at concentrations ranging from 0-2400 μM were mixed with 1 μM STK-3 peptide substrate (CisBio) in a buffer solution containing 50 mM MOPS (pH 7), 10 mM magnesium acetate, 0.025% NP40 (Sigma), 1.5% Glycerol, 1 mM DTT, 0.5 mg/mL BSA, and 0.1% DMSO. The reaction was initiated by the addition of activated ASK1 to a final concentration of 2 nM, with a final reaction volume of 100 μL. After a three-hour incubation, 100 μL of 2×KinEASE quenching-detecting reagent (CisBio) were added, and the mixture was incubated for an additional 1.5 hours. Product formation was measured using time-resolved FRET on a Tecan Infinite M1000 plate reader using an excitation wavelength of 317 nM and emission wavelengths of 620 nm and 665 nm. The ratio of fluorescence at 665 nm to that at 620 nm was the measure of product formation.

References

1. Otwinowski Z, Minor W. Processing of X-Ray diffraction data collected in oscillation mode. *Methods Enzymol*. 1997;276:307-326.

2. Adams PD, Afonine PV, Bunkoczi G, et al. PHENIX: a comprehensive Python-based system for macromolecular structure solution. *Acta Crystallogr D Biol Crystallogr*. 2010;66(Pt 2):213-221.

3. Emsley P, Cowtan K. Coot: model-building tools for molecular graphics. *Acta Crystallogr D Biol Crystallogr*. 2004;60(Pt 12 Pt 1):2126-2132.